General Disclaimer

One or more of the Following Statements may affect this Document

- This document has been reproduced from the best copy furnished by the organizational source. It is being released in the interest of making available as much information as possible.

- This document may contain data, which exceeds the sheet parameters. It was furnished in this condition by the organizational source and is the best copy available.

- This document may contain tone-on-tone or color graphs, charts and/or pictures, which have been reproduced in black and white.

- This document is paginated as submitted by the original source.

- Portions of this document are not fully legible due to the historical nature of some of the material. However, it is the best reproduction available from the original submission.

Produced by the NASA Center for Aerospace Information (CASI)

NASA TECHNICAL MEMORANDUM

NASA TM-77719

DYNAMIC PROPERTY STUDIES OF STERLING
ENGINES

Y. Tani, M. Seibara, K. Takenai, and
W. Yamaguchi

STANDARD TITLE PAGE

1. Report No. NASA TM- 77719	2. Government Accession No.	3. Recipient's Catalog No.
4. Title and Subtitle DYNAMIC PROPERTY STUDIES OF STERLING ENGINES		5. Report Date FEBRUARY 1984
		6. Performing Organization Code
7. Author(s) Y. Tani, M. Seibara, K. Takenai, and W. Yamaguchi		8. Performing Organization Report No.
		10. Work Unit No.
9. Performing Organization Name and Address SCITRAN Box 5456 Santa Barbara, CA 93108		11. Contract or Grant No. NASw- 3542
		12. Type of Report and Period Covered Translation
12. Sponsoring Agency Name and Address National Aeronautics and Space Administration Washington, D.C. 20546		14. Sponsoring Agency Code

15. Supplementary Notes

Translation of "Sutaringu enjin no doryoku tokusei shiken",
Nihon Kikai Gakkai Koen Ronbunshu, No. 810-5, pp. 132-4

16. Abstract

A description is given of the results
of dynamic property tests that were carried out
using a trial-produced prototype of a
50 KW Sterling engine. The features of
the engine are shown graphically. It
is found that a high thermal efficiency
is found in the low rotation region.

17. Key Words (Selected by Author(s))	18. Distribution Statement Unclassified and Unlimited	
19. Security Classif. (of this report) Unclassified	20. Security Classif. (of this page) Unclassified	21. No. of Pages 10	22. Price

DYNAMIC PROPERTY STUDIES ON STERLING ENGINES*

Yukio Tani**, Maraseio Seibara**, Kanewa
Takenai**, and Wamei Yamaguchi**

1.   Introduction

There has been a recent demand for sterling engines as   /132***
future fuel engines because of their high efficiency, fuel
diversity, low toxicity, etc. Progress has been particularly
strong in the U.S. on the development of sterling engines
because of their low energy consumption. On the other hand,
several Japanese research institutes and companies have been
carrying out studies on sterling engines. However, there
are few experimental reports on the dynamic properties of
the engine in the test results on theoretical analyses and
component features.

We will report here on the results of dynamic property
tests that were carried out using a trial-produced prototype
of a 50 KW sterling engine.

2.   Engine Summary

The features of the trial-produced engine are shown in
Table 1 and its cross section is shown in Figure 1.

TABLE 1. Features of Sterling Engine

|	
Operating gas	He gas
Fuel	Kerosene
Piston type	Double acting
Number of air cylinders	4
Bore x stroke	φ68 x 52
Heater tube temperature	750°C
Coolant temperature	20°C
Output pick up device	Rotating swash plate engine
Axial sealing method	Sliding seal
Output control method	Minimum pressure control method
Combustion method	Ultrasonic wave fogging combustion method
Air preheater	Multitube type
High temperature heat exchanger	SUS tube type
Low temperature heat exchanger	Shell and tube type
Regenerative materials	SUS net
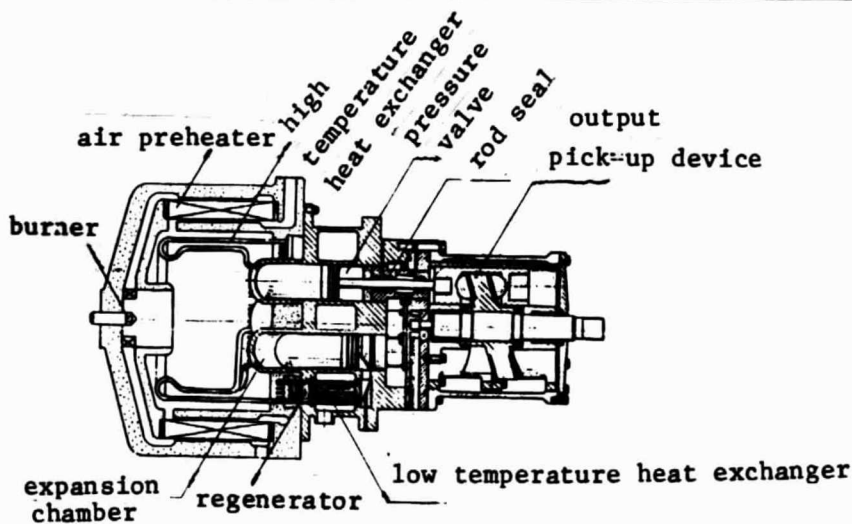
Figure 1. Cross section of Sterling Engine.

This engine is the same as that reported previously [1]. It uses the 4 air cylinder double-acting system and has 4 pistons in a circle at a distance of 90°. The output is picked up by a rotating swash plate engine. The fuel is kerosene and the operating gas is helium. Output control is carried out by control of the minimum pressure of the operating gas with a check valve. Moreover, a sliding seal is used as the rod seal.

3.   Testing Method

In this test the dynamic measurements of the engine were carried out by controlling the r.p.m. using a direct current electric dynamometer. Friction loss of the piston ring, rod seal, and output pick-up device was determined from the amount of heat transmitted to the coolant. Heat loss of the exhaust was computed from the air ratio, which was determined from gas analysis, and the exhaust temperature. The amount of heat exchanged by the air preheater was determined from the flow and temperature of air used in combustion. The temperature control of the heater tube was carried out by setting up 16 CA thermocouples on the outside of the tube and controlling the amount of fuel fed so that the mean temperature would be constant. Furthermore, extra blowers and fuel pumps were used in the tests and were operated separately.

4. Test Results and Considerations

The engine property curves obtained during these tests and the equivalent efficiency curves are shown in Figure 2. Axial output is shown with regard to an operating gas minimum pressure of 10 MPa (during total load), 6 MPa and 4 MPa. The mean temperature of the heater tube was 750°C and the operating gas pressure ratio at this time was approximately 1.8.

The maximum output obtained in these tests was 57 KW (71P)/ 2,500 r.p.m. and the maximum efficiency was 31% (fuel consumption rate of 196 g/psH)/700 r.p.m. The maximum torque was 30 kg^{-m}/500 r.p.m. Furthermore, the torque in the low rotation region was practically flat up to 200 r.p.m. and smooth operation was possible. Moreover, this engine showed a higher efficiency in the low rotation region.

4-1) Thermal Calculations

The thermal calculation chart during maximum efficiency is shown in Figure 3. Approximately 65% of the thermal energy of the exhaust is recovered by the air preheater in this engine. Exhaust loss is very low at 15%. Heat leaks show an almost constant value under a constant heater tube temperature. The measures are approximately 3 KW through the sealing walls, etc. to the coolant and approximately 1KW from the heating furnace walls, etc. to the atmosphere. Seal loss is due to fraction loss of the piston ring and the rod seal.

4-2 Effects of R.P.M.

The correlation between the efficiency of the entire unit and each section during engine total load and the number of r.p.m.s is shown in Figure 4. Thermal efficiency η_{Gross} is at the maximum with approximately 700 r.p.m. and decreases on the high rotation side. Burner efficiency η_B is at a maximum near 1,500 r.p.m. (fuel input of 140 KW) and shows a tendency to be lower than the reduction in the heat efficiency of the air preheater and high temperature heat exchanger on a higher rotation side. The illustrated efficiency η_{ind} is approximately 5.2% in the low rotation

4

region and decreases with an increase in the r.p.m.
The Carnot efficiency shown in the figure is computed from
$\eta_{car}=(TH-TC)/TH$ from the temperature TH of the expansion chamber
walls and the pressure chamber temperature TC. The curve
coefficient η_{dia} is the ratio of the illustrated efficiency
to the Carnot efficiency. The curve coefficient appears
to decrease in the high rotation region because of pressure
loss of the operating gas. Moreover, the engine
efficiency η_m is at a maximum near 1,000 r.p.m. The reduction
in the engine efficiency at the high rotation region appears to
be due to the fact that in constrast to the decrease in the rate
at which the output increases with r.p.m., friction
loss of the seal and output pick up device increases almost
proportionally to the r.p.m.

4-3) Effect of Operating Gas Pressure

The correlation between the output and operating gas
pressure with 1,000 r.p.m. is shown in Figure 5 and the correlation
between the efficiency of the total unit and each section
and the operating gas pressure is shown in Figure 6. Thermal
efficiency shows a tendency to increase with an increase in
the operating gas pressure. However, the rate of increase
decreases at approximately 10 MPa. Burner efficiency decreases
on the low pressure side because the heat leak from the   /134
heating furnace is practically constant. The illustrated
efficiency decreases slightly with an increase in operating
gas pressure. This is due to the reduction in Carnot
efficiency. The reduction in the Carnot efficiency occurs
for the following reasons. (1) The input to the operating
gas increases almost proportionally to the operating
gas pressure and therefore, the operating gas temperature of
the expansion chamber decreases at a constant heater tube
temperature. (2) The amount of heat transmitted by the low
temperature heat exchanger increases with an increase in pressure
and therefore, the temperature of the operating gas in
the pressure chamber increases. Engine efficiency shows
a tendency to decrease in the low rotation region and
increase monotonously with an increase in pressure. This
is due to the fact that the friction loss of the driving
section and seal to the illustrated output is very high

5

on the low pressure side. Moreover, the friction loss of the
seal is proportional to the operating gas pressure
and the high pressure side and the driving section loss is
proportional to approximately 1/2 this pressure. Therefore,
the total of both friction losses decreases relative to the
illustrated output.

4-4 Effect of Heater Tube Temperature

The effect of the heater tube temperature
on output and efficiency is shown in Fgiure 7. Here the case
where the temperature is varied under each operation condition
in relation to the maximum output and maximum efficiency
is shown. The efficiency increased 1.5% and output increased
5 KW with each 50 °C increase in the heater tube temperature
within the range of this test. This is obviously due to
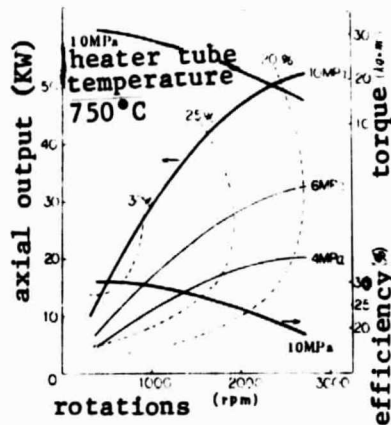the increase in the Carnot efficiency.

Figure 2   Engine Property Curves and Equivalent
Efficiency Curves

burner efficiency: $\eta_b = \frac{C+D+E+F}{Q}$

illustrated efficiency: $\eta_{id} = \frac{D+E+F}{C+D+E+F}$

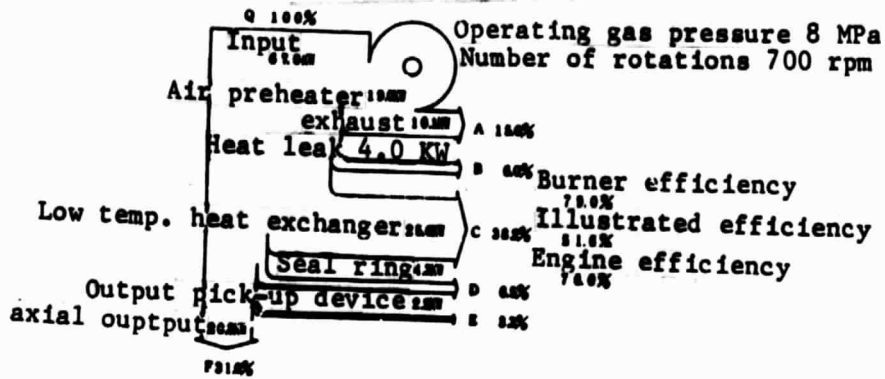engine efficiency: $\eta_e = \frac{F}{D+E+F}$
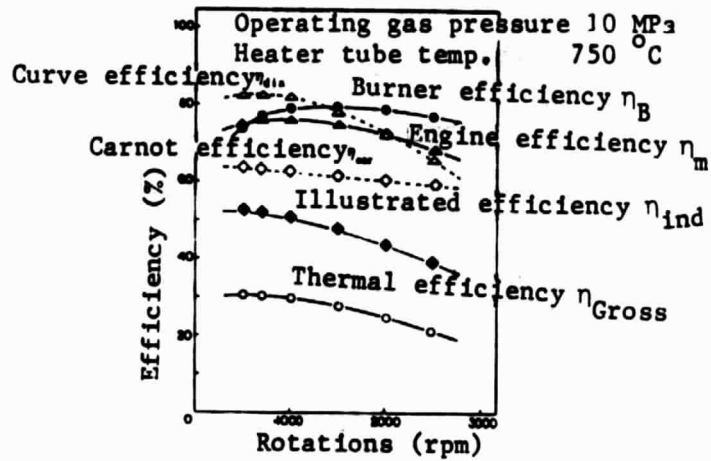
Figure 3.   Thermal computation chart

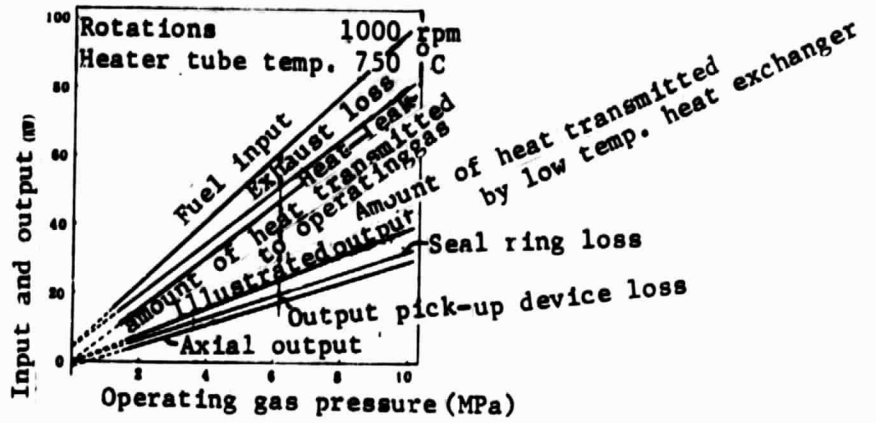Figure 4.   Correlation between efficiency and R.P.M.

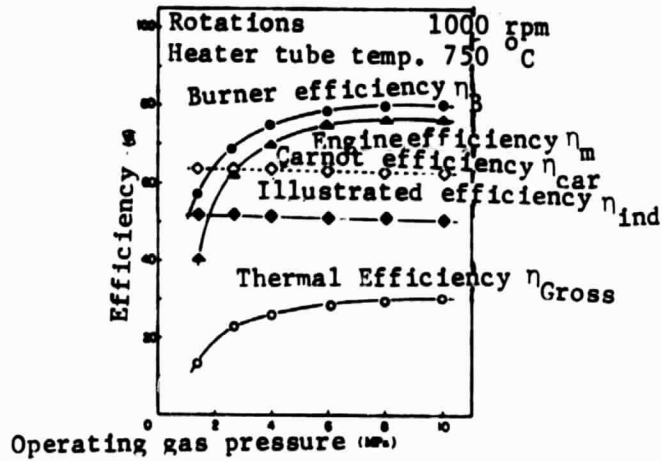Figure 5. Correlation between input and output and
operating gas pressure.

Figure 6. Correlation between efficiency and operating
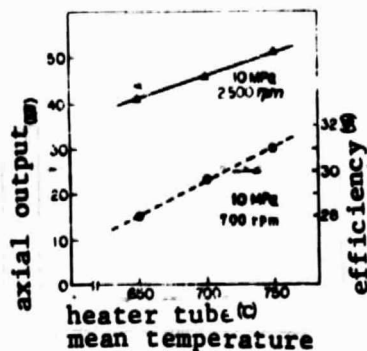gas pressure.

8

Figure 7. Effect of heater tube temperature

5. Conclusion

Knowledge on the basic dynamic properties of the sterling engine was obtained from these tests. The particularly important points are as follows: (1) Torque is very large in the low rotation region and smooth operation is possible. (2) A high thermal efficiency is shown in the low rotation region. Moreover, in this test the maximum output was 52 KW and the maximum efficiency was 31%. However, it was also shown that improved efficiency and output can be anticipated with an increase in the operating gas pressure and the temperature. It is a known fact that when hydrogen is used as the operating gas, the output is increased 1.5 times in comparison to the case of helium (2). Therefore, we will also carry out tests on the use of hydrogen.

In conclusion we would like to express our thanks to the Ministry of International Trade and Industry Industrial Technology Agency for their help in making this study possible, and to the Tokyo Engineering University for their assistance.

Bibliography

[1] Ishizaki, Tani, and Haramura: "Experimental Research on
    the Sterling Engine", *Nihon Kikai Gakkai Ronbun Shu*,
    No. 790-16 (10/1979).

[2] Roy C. Tew, et al.: SAE Paper 790327(1979).